Supplementary Information (SI) for Chemical Science.

Supporting Information

Ethanol-assisted synthesis of titanium-rich TS-1 zeolite: a new hexa-coordinated Ti site for efficient propylene epoxidation

Dapeng Hao,[ab] Xintong Li,[c] Guangyuan He,[d] Risheng Bai,[a] Yang Bai,[a] Tianjun Zhang,[e] Lisu Bai,[ab] Jialiang Li,[ab] Qiang Zhang,[ab] Donghai Mei,[ad] Zhaochi Feng,*[f] Jihong Yu*[ab]

[a]State Key Laboratory of Inorganic Synthesis and Preparative Chemistry, College of Chemistry, Jilin University, 2699 Qianjin Street, Changchun 130012, P. R. China

[b]International Center of Future Science, Jilin University, 2699 Qianjin Street, Changchun 130012, P. R. China

[c]Shanghai Key Laboratory of Green Chemistry and Chemical Processes, School of Chemistry and Molecular Engineering, East China Normal University, Shanghai 200062, P. R. China

[d]School of Materials Science and Engineering, Tiangong University, Tianjin 300387, P. R. China

[e]State Key Laboratory of New Pharmaceutical Preparations and Excipients, Key Laboratory of Medicinal Chemistry and Molecular Diagnosis of the Ministry of Education, College of Chemistry and Materials Science, Hebei University, 071002, P. R. China

[f]State Key Laboratory of Catalysis, Dalian Institute of Chemical Physics, Chinese Academy of Sciences, 457 Zhongshan Road, Dalian, 116023, P. R. China

*Corresponding Authors: Zhaochi Feng: zcfeng@dicp.ac.cn； Jihong Yu: jihong@jlu.edu.cn

Contents

1 Experimental Sections and Characterizations

1.1 Chemicals and reagents

All chemicals and reagents were supplied by commercial suppliers and used without further purification: tetraethylorthosilicate (TEOS, Sinopharm Chemical Reagent Company, 28.4 wt% as SiO_2), tetrapropylammonium hydroxide solution (TPAOH, Kente Catalysts Inc, 25 wt%), tetrabutyl orthotitanate (TBOT, Sinopharm Chemical Reagent Company, 98%), ethanol (C_2H_5OH, Sinopharm Chemical Reagent Company, 99%), methanol (CH_3OH, Sinopharm Chemical Reagent Company, 99%), hydrogen peroxide (H_2O_2, Sinopharm Chemical Reagent Company, 30%), cerium(IV) sulfate ($Ce(SO_4)_2$, Sinopharm Chemical Reagent Company, 99%), propylene (C_3H_6, 99.99%, Shanghai WOGE Gas Equipment CO.,Ltd).

1.2 Synthesis

Synthesis of TS-1-E-80-170

TS-1-E-80-170 samples were synthesized through a two-step hydrothermal route under static conditions from the starting gels with the molar compositions of $1.0SiO_2$: $0.033TiO_2$: 0.2TPAOH: $1.5C_2H_5OH$: $9H_2O$. Typically, deionized water and TPAOH (25 wt%) were mixed completely, and TEOS was added to the mixture of H_2O and TPAOH then under stirring for 4 h, giving rise to the solution A. Tetrabutyl orthotitanate (TBOT) was dissolved in ethanol under stirring for 4 h, forming solution B. Then solution B was added to solution A dropwise and the mixture was stirred for another 2 h. Subsequently, the gel mixture was transferred into a Teflon-lined stainless-steel autoclave. The crystallization process was conducted at 80 °C for 48 h and then at 170 °C for 0-168 h. The as-synthesized solid products were centrifuged, washed with water three times and dried at 80 °C in an oven overnight. Finally, the samples were calcined at 550 °C for 6 h. The as-synthesized TS-1 samples were denoted as TS-1-E-80-170, where 80 and 170 represent the temperature of two-step crystallization.

Synthesis of TS-1-C-80-170

TS-1-C-80-170 was prepared with the same synthesis procedure as described above except that ethanol was evaporated with an infrared lamp.

Synthesis of TS-1-E-170

TS-1-E-170 was prepared with the same synthesis procedure as described above but through a one-step hydrothermal route, the crystallization process was conducted at 170 °C.

1.3 Characterizations

The crystal morphology was measured by scanning electron microscopy (SEM) by a JEOL-7800 electron microscope, transmission electron microscopy (TEM) and high-resolution TEM (HRTEM) at 200 kV using a Tecnai F20 electron microscope. The crystallinity and phase purity of the samples were characterized by powder X-ray diffraction (PXRD) on a BRUKER D8 ADVANCE with Cu Kα radiation ($\lambda = 1.5418$ Å). The Si/Ti ratios were determined by inductively coupled plasma (ICP) analyses carried out on an Agilent 725 ICP instrument. Nitrogen adsorption/desorption measurements were carried out on a BSD-660 at 77.35 K after the samples were degassed at 350°C under vacuum. ^{29}Si solid-state MAS NMR experiments were performed on a Bruker Avance Neo 600 MHz spectrometer at a magnetic field strength of 14.1 T. X-ray photoelectron spectroscopy (XPS) was performed with an ESCALAB 250 X-ray photoelectron spectrometer using Al as the excitation source. Ti species were investigated by UV-visible diffuse reflectance spectroscopy (UV-vis) over a range of 200 to 600 nm using a SHIMADZU U-4100 instrument. The baseline correction was carried out with powder $BaSO_4$. Fourier transform infrared (FT-IR) spectra were recorded on a BRUKER vertex 80v, and samples were pelleted with KBr powder before testing. Thermal gravimetric (TG) analyses were performed using a TA TGA Q500 at temperatures ranging from room temperature to 800 °C at a heating rate of 10 °C min^{-1}. Nitrogen adsorption/desorption measurements were carried out on a Micromeritics 2020 analyzer at 77 K after the samples were degassed at 350 °C under vacuum. Ultraviolet Raman resonance (UV Raman) spectra were recorded on a DL-2 Raman spectrometer using the 244 nm, 257 nm, 266 nm, and 325 nm line of a He-Ge laser as the excitation source and a Princeton CCD as the detector. The data of X-ray absorption near-edge structure (XANES) and extended X-ray absorption fine structure (EXAFS) were collected at room temperature in the fluorescent mode with a Lytle detector at beamline BL14W1 of the Shanghai Synchrotron Radiation Facility (SSRF, China).

1.4 Density functional theory calculations

Periodic density functional theory (DFT) calculations were conducted utilizing the CP2K code, employing a mixed Gaussian and planewave basis sets. Core electrons were represented using norm-conserving Goedecker-Teter-Hutter pseudopotentials, [1] and the valence electron wavefunction was expanded in a double-zeta basis set with polarization functions,[2] along with an auxiliary plane wave basis set with an energy cutoff of 360 Ry. The Perdew, Burke, and Enzerhof (PBE) generalized gradient approximation exchange-correlation functional was utilized. Test calculations demonstrated that the total energy change of the reactive system was negligible (<0.01 eV) when employing a maximum force convergence criterion of 0.001 hartree/bohr. All geometric optimization was optimized using the Broyden-Fletcher-Goldfarb-Shanno (BGFS) algorithm with self-consistent field (SCF) convergence criteria of 1.0×10^{-8} atomic units. The DFT-D3 scheme with an empirical damped potential term was incorporated into the energies obtained from the exchange-correlation functional in all calculations.[3] The vibrational frequencies are calculated in the framework of the localized harmonic oscillator approximation with a displacement of 0.01 Å. In the vibrational frequency calculation, only the atoms of hexa-coordinated titanium site were considered while other atoms on the TS-1 zeolite framework were fixed. The TS-1 zeolite structure was modelled with the size parameters of $20.0220 \times 19.8990 \times 13.3830$ Å^3, $\alpha = \beta = \gamma = 90°$. As the T7 site was regarded as one of the preferable positions for the Ti atoms in the MFI framework,[4-5] we chose the T7 sites to construct the hexa-coordinated titanium species.

2 Catalytic Tests

propylene epoxidation

All the shaped catalysts used in the reaction were ground to powder to eliminate the diffusion constrains. In a typical run, 0.03 g catalyst, 0.03 mol H_2O_2 (30 wt% aqueous solution) and 10 mL CH_3OH were added into a stainless-steel autoclave reactor equipped with a Teflon-inner. The propylene was then kept into the reactor at a constant pressure of 0.4 MPa, after purging the air inside by propylene for three times. After stirring vigorously at 313 K for 1 h, the reactor was cooled down with ice water and then depressurized slowly. The reaction solution was separated for GC and titration analysis.

The reaction products were analyzed by a Gas Chromatograph (Shimadzu 2014, FID detector, Rtx-Wax capillary column) and the obtained products were further confirmed by a GC-MS (Agilent 6890 series GC system, 5937 network mass selective detector). The remaining amount of H_2O_2 was determined by the titration method with 0.05 M $Ce(SO_4)_2$ aqueous solution. Propylene oxide (PO) is the target product and propylene glycol (PG) and its monomethyl ethers (MME) are byproducts. The conversion of H_2O_2 ($X(H_2O_2)$), selectivity of PO ($S(PO)$), and yield of PO ($Y(PO)$) were calculated using formula (1) to (3), respectively. Here $n_o(H_2O_2)$ and $n(H_2O_2)$ are the initial and final molar number of H_2O_2, respectively; $n(PO)$, $n(MME)$, and $n(PG)$ are the molar number of the PO, MME, and PG, respectively.

$$X(H_2O_2) = (1-n(H_2O_2)/n_o(H_2O_2)) \times 100\% \quad (1)$$

$$S(PO) = n(PO)/(n(PO) + n(MME) + n(PG)) \times 100\% \quad (2)$$

$$Y(PO) = n(PO)/n_o(H_2O_2) \times 100\% \quad (3)$$

$$U(H_2O_2) = n(PO)/(S(PO) \times n_o(H_2O_2) \times X(H_2O_2)) \times 100\% \quad (4)$$

Catalyst regeneration and test.

The TS-1 zeolites catalysts were regenerated by a calcination cycle. The samples were calcined at 550 °C for 6 h after four times cycles.

3 Supplementary Figures and Tables

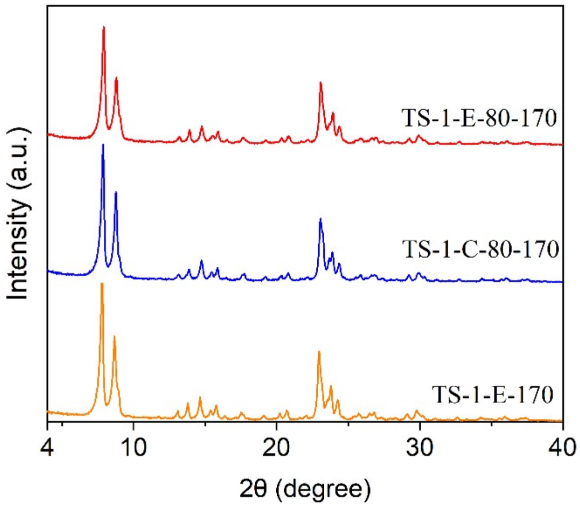

Fig. S1 XRD patterns of TS-1-E-80-170, TS-1-C-80-170 (both crystallized at 80 °C for 48 h and then crystallized at 170 °C for 15 h), and TS-1-E-170 (directly crystallized at 170 °C for 63 h).

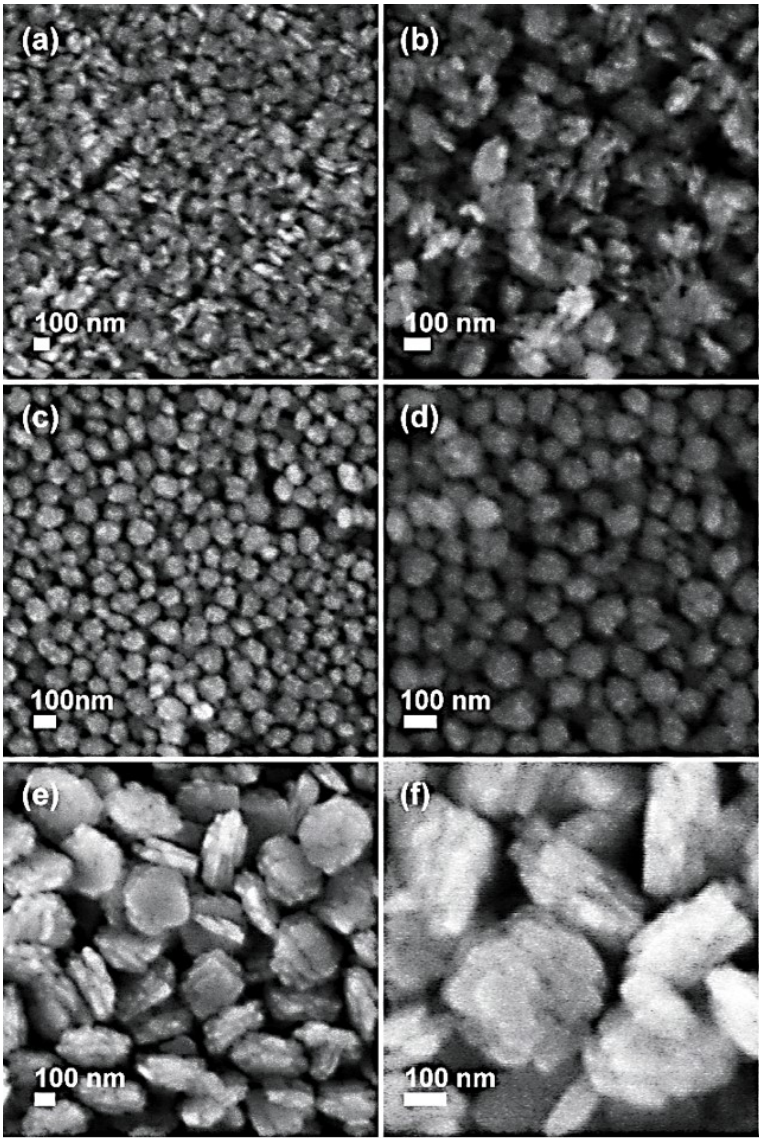

Fig. S2 SEM images of (a, b) TS-1-E-80-170, (c, d) TS-1-C-80-170, and (e, f) TS-1-E-170.

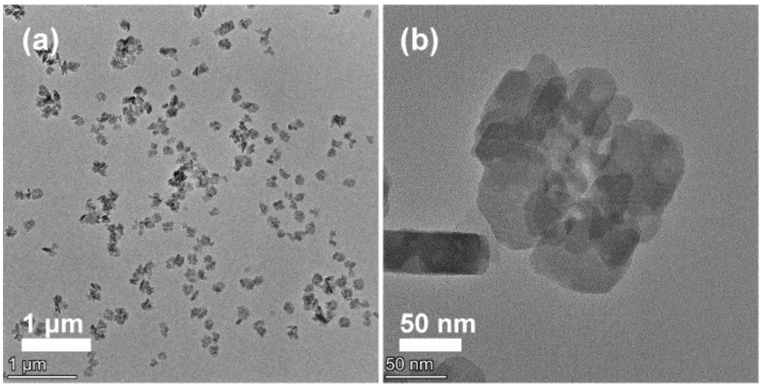

Fig. S3 (a, b) TEM images of TS-1-E-80-170.

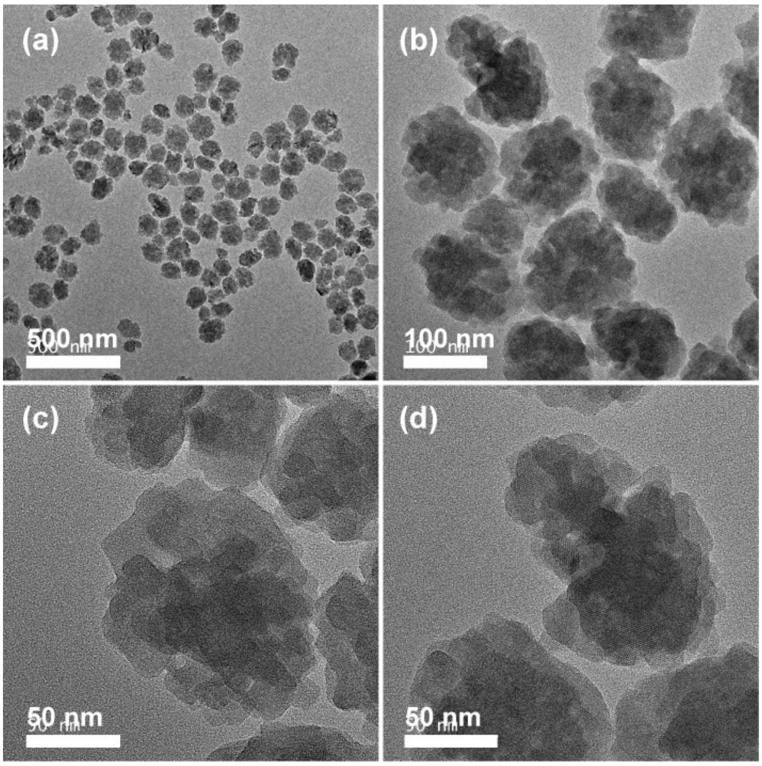

Fig. S4 (a-d) TEM images of TS-1-C-80-170.

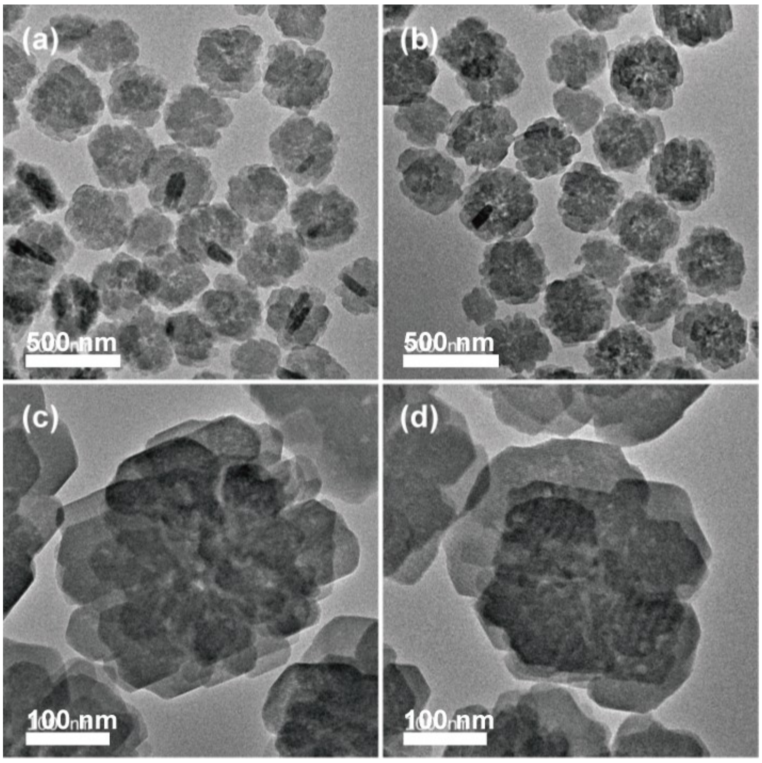

Fig. S5 (a-d) TEM images of TS-1-E-170.

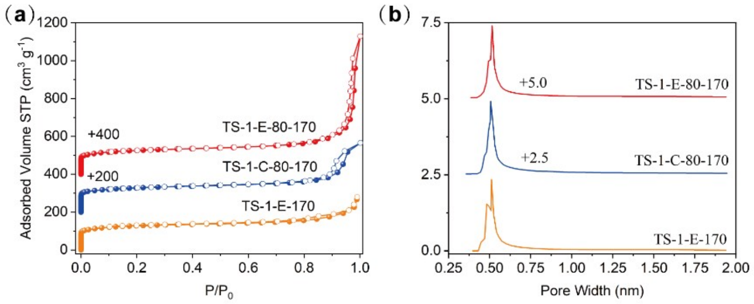

Fig. S6 (a) N_2 adsorption/desorption isotherms, (b) Horvath-Kawazoe (H-K) pore size distributions of TS-1-E-80-170, TS-1-C-80-170, and TS-1-E-170.

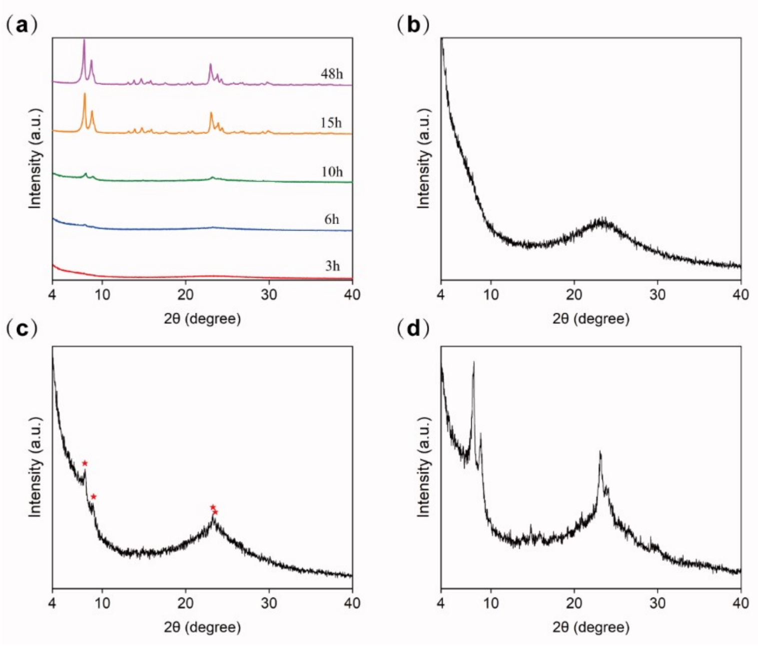

Fig. S7 XRD patterns of TS-1-E-80-170 samples crystallized at 80 °C for 48 h and further crystallized at 170 °C for (a) different time (3 - 48 h), (b) 3 h, (c) 6 h, and (d) 10 h.

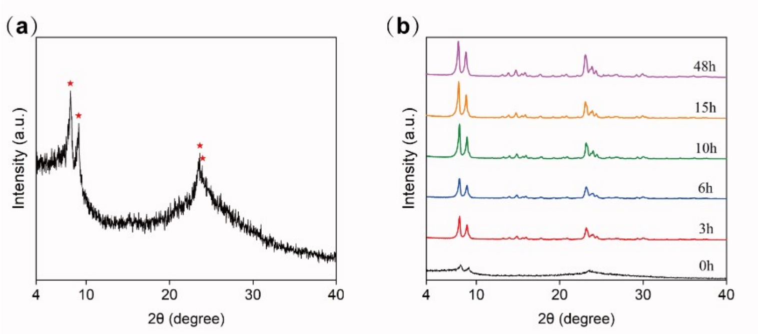

Fig. S8 XRD patterns of TS-1-C-80-170 samples (a) crystallized at 80 °C for 48 h and (b) further crystallized at 170 °C for different time.

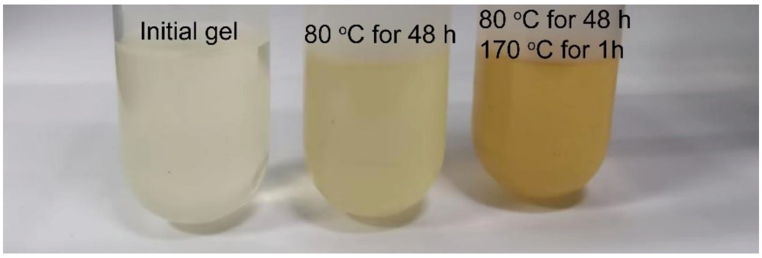

Fig. S9 Photograph of TS-1-E-80-170 samples at different crystallization stages including initial gel, initial gel crystallized at 80 °C for 48 h, and initial gel crystallized at 80 °C for 48 h then further crystallized at 170 °C for 1 h.

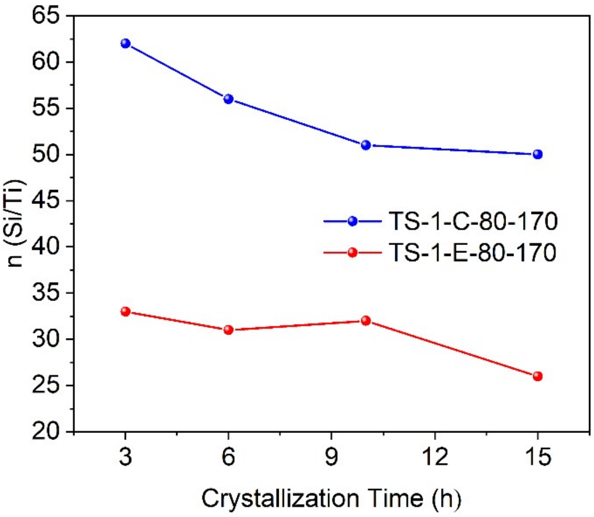

Fig. S10 n(Si/Ti) determined by ICP of TS-1-E-80-170 and TS-1-C-80-170 crystallized at 80 °C for 48 h and then crystallized at 170 °C for different time.

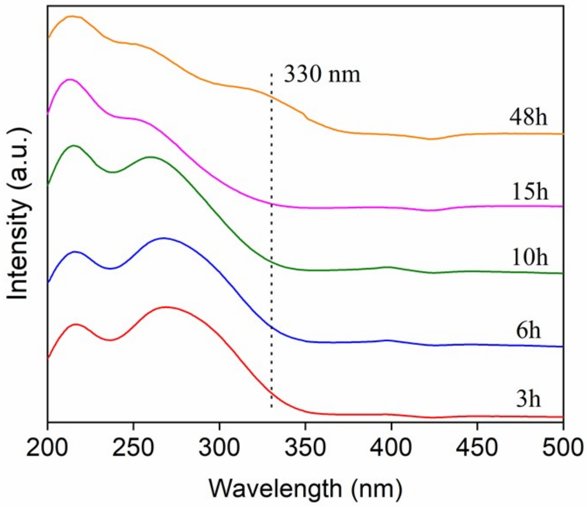

Fig. S11 UV-vis spectra of TS-1-E-80-170 crystallized at 80 ℃ for 48 h and then crystallized at 170 ℃ for different time.

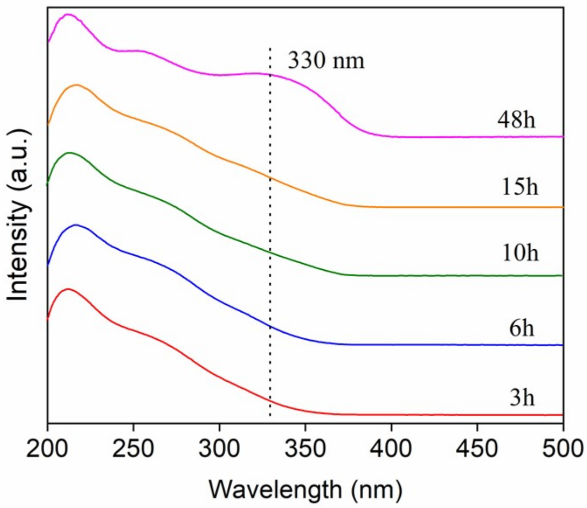

Fig. S12 UV-vis spectra of TS-1-C-80-170 crystallized at 80 ℃ for 48 h and then crystallized at 170 ℃ for different time.

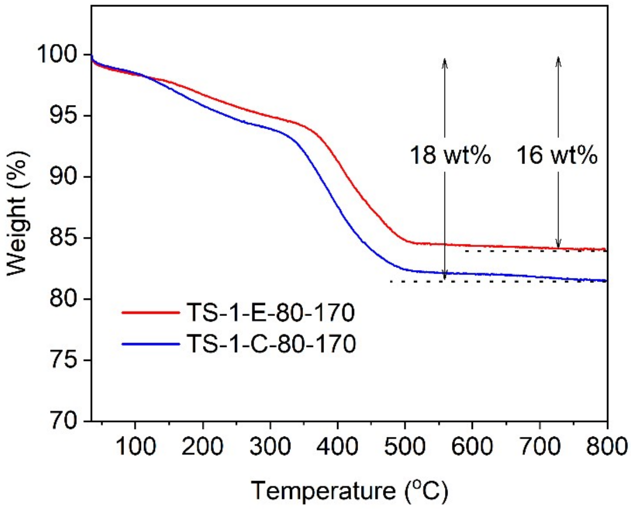

Fig. S13 TG curves of as-made TS-1-E-80-170 and TS-1-C-80-170.

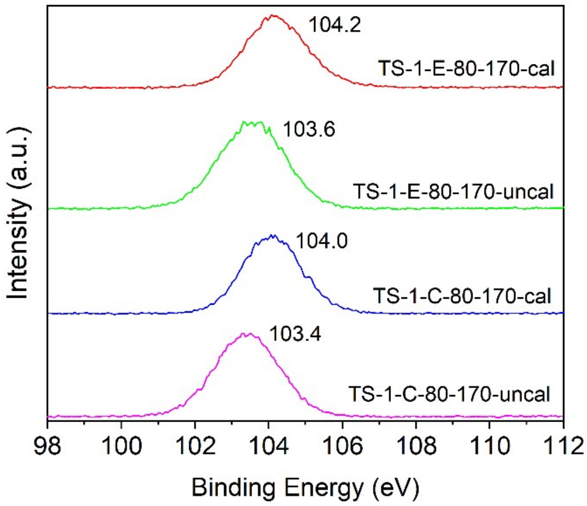

Fig. S14 XPS spectra of Si 2p of TS-1-E-80-170 and TS-1-C-80-170 before and after calcination.

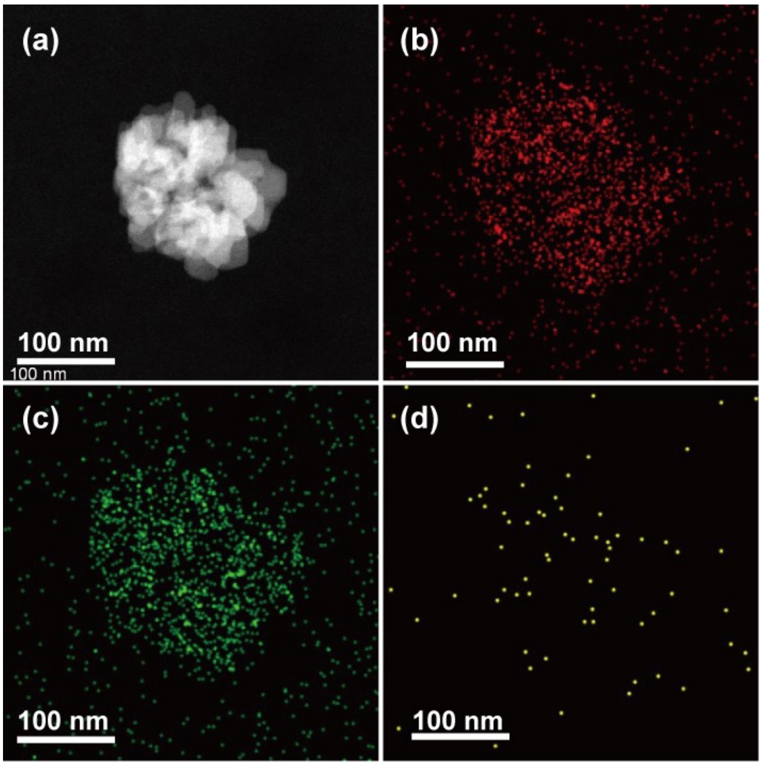

Fig. S15 (a) STEM image and elemental mappings of (b) O, (c) Si, and (d) Ti for TS-1-E-80-170.

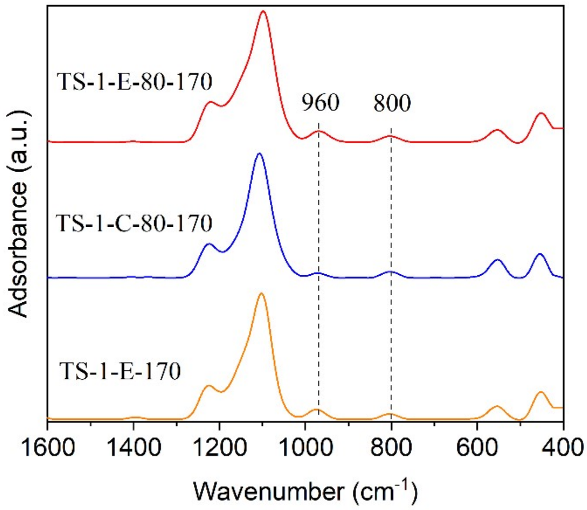

Fig. S16 Infrared absorption spectra of TS-1-E-80-170, TS-1-C-80-170, and TS-1-E-170.

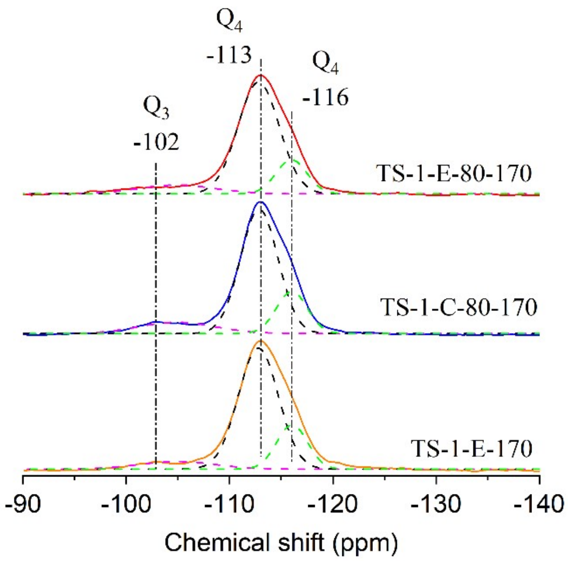

Fig. S17 ^{29}Si MAS NMR spectra of TS-1-E-80-170, TS-1-C-80-170, and TS-1-E-170.

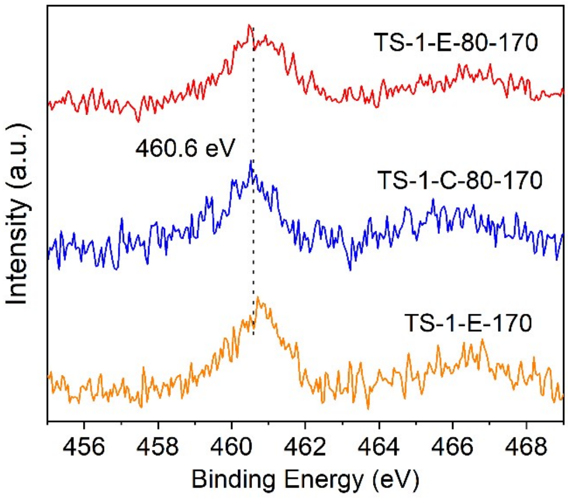

Fig. S18 Ti XPS spectra of TS-1-E-80-170, TS-1-C-80-170, and TS-1-E-170.

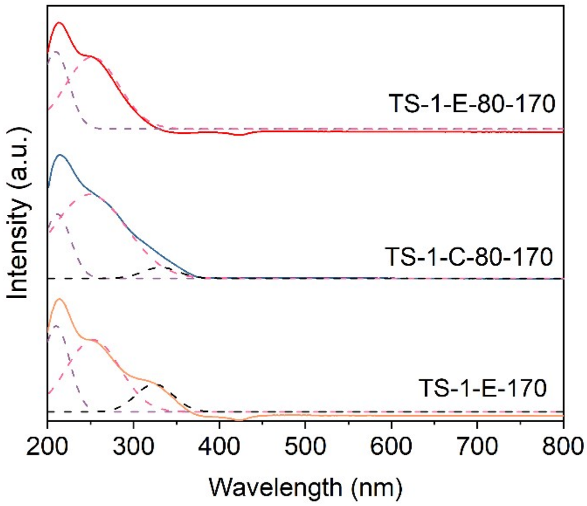

Fig. S19 UV-vis spectra of TS-1-E-80-170, TS-1-C-80-170, and TS-1-E-170.

The total UV-vis spectra presented in Fig. S18 of the three catalysts are de-convoluted based on the Ti species identified and the de-convoluted spectra are also included in the Figure.

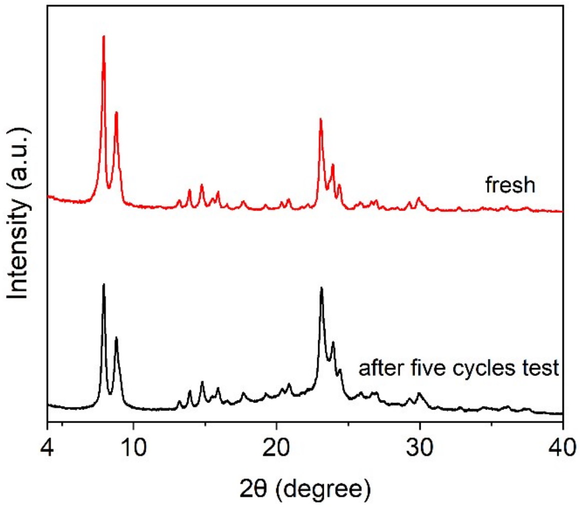

Fig. S20 XRD patterns of fresh TS-1-E-80-170 and TS-1-E-80-170 after five cycles test.

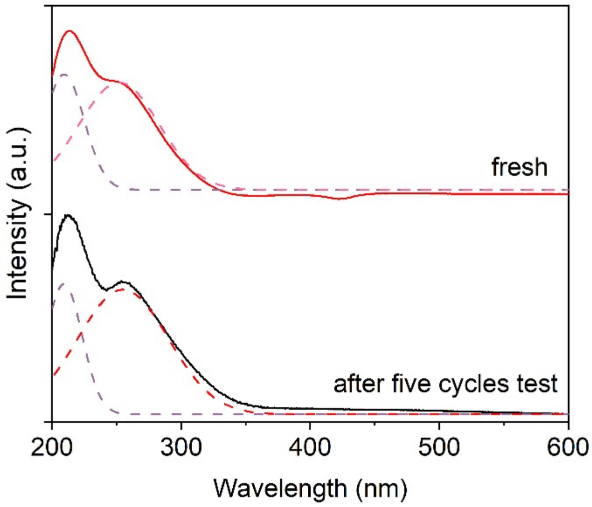

Fig. S21 UV-vis spectra of fresh TS-1-E-80-170 and TS-1-E-80-170 after five cycles test.

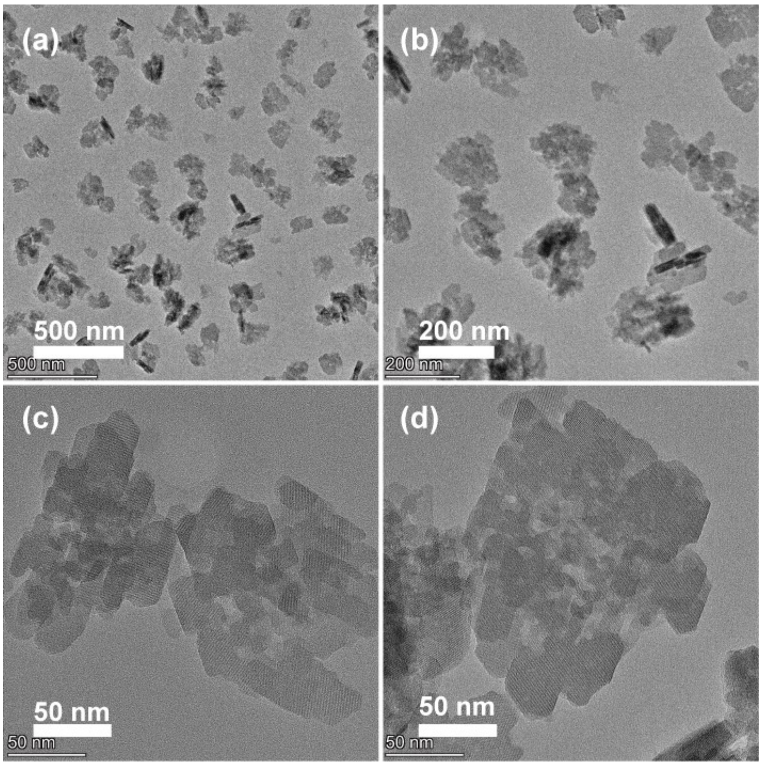

Fig. S22 (a-d) TEM images of TS-1-E-80-170 after five cycles test.

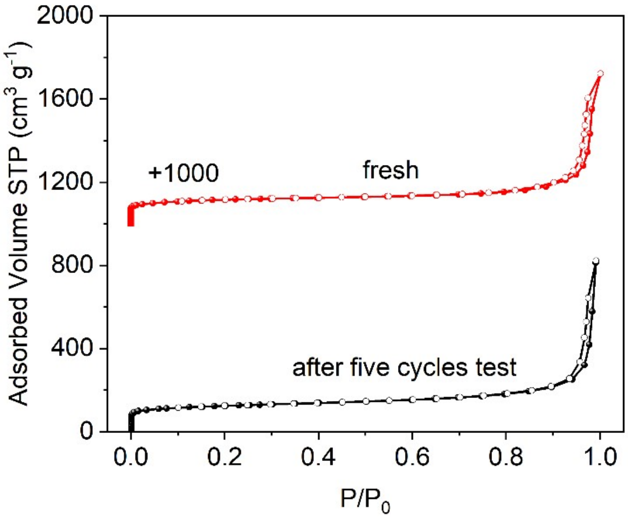

Fig. S23 N_2 adsorption/desorption isotherms of fresh TS-1-E-80-170 and TS-1-E-80-170 after five cycles test.

Table S1: Textural properties of TS-1 samples.

	$S_{BET}{}^a$ (m^2 g^{-1})	$S_{micro}{}^b$ (m^2 g^{-1})	$S_{ext}{}^b$ (m^2 g^{-1})	$V_{total}{}^c$ (cm^3 g^{-1})	$V_{micro}{}^b$ (cm^3 g^{-1})	$V_{meso}{}^d$ (cm^3 g^{-1})
TS-1-E-80-170	466	333	133	0.97	0.14	0.83
TS-1-C-80-170	476	345	131	0.55	0.14	0.41
TS-1-E-170	476	354	122	0.43	0.14	0.29
TS-1-E-80-170 after recycle test	467	304	163	1.26	0.13	1.13

$^a S_{BET}$ (total surface area) is calculated by applying the BET equation using the linear part ($0.05 < P/P_0 < 0.30$) of the adsorption isotherm; $^b S_{micro}$ (micropore area), S_{ext} (external area), and V_{micro} (micropore volume) calculated using the *t*-plot method; ^{c} Total pore volume at $P/P_0 = 0.99$; $^d V_{meso} = V_{total} - V_{micro}$.

Table S2: Relative crystallinities of TS-1 samples crystallized at 80 ℃ for 48 h and then further crystallized at 170 ℃ for different time.

	0 h (%)	3 h (%)	6 h (%)	10 h (%)	15 h (%)	48 h (%)
TS-1-E-80-170	0	0	14.4	22.5	98.6	100
TS-1-C-80-170	3.9	25.9	28.3	32.8	33.4	100

The relative crystallinities are calculated based on the peak area of the three strongest peaks ($2\theta=23.1°$, 24.0°, 24.5°) in the XRD pattern. The relative crystallinity=$\sum A/\sum Ar\times 100\%$.

Table S3: The assignment of experimental Raman peaks, along with the elucidation of coordination structures for the Ti(OH_2)(OSi)$_3$(OSiOH)$_2$ species identified using DFT calculations.

DFT calculated Raman Peak (cm^{-1})	Experimentally observed Raman Peak (cm^{-1})	Raman peak assignment	Coordination number	Bonds
525	524	Ti-O-Si-OH wagging	6	Ti-OH_2(1) Ti-O-Si(3) Ti-O-Si-OH(2)
1098	1100	Ti-O-Si-OH wagging		

Table S4: Assignment of experimental Raman peaks and coordination structures for previously reported Ti species based on DFT calculations.

DFT calculated Raman Peak (cm^{-1})	Experimentally observed Raman Peak (cm^{-1})	Raman peak assignment	Ti species	Coordination number	Bonds
715	695	Ti-O symmetric stretch	$Ti(H_2O)_2(OH)_2(OSi)_2$	6	$Ti-OH_2(2)$ Ti-O-Si(2) Ti-OH(2)
493	490	Ti-O-Si bending	Ti-IV ($TiOH(OSi)_3$)	4	Ti-O-Si(3) Ti-OH(1)
1130	1125	Ti-O-Si stretching			
511	510	Ti-O-H wagging	Ti-V ($Ti(OH)_2(OSi)_3$).	5	Ti-O-Si(3) Ti-OH(2)
680	685	Ti-O-H rocking			
1119	1125	Ti-O-Si stretching			
440	441	Ti-O-H wagging	Ti-VI ($Ti(OH)_4(OSi)_2$).	6	Ti-O-Si(2) Ti-OH(4)
709	705	Ti-O-H rocking			
1119	1125	Ti-O-Si stretching			
1339	1342	Si-O-H rocking			

Table S5: Epoxidation of propene over different TS-1 samples.

	H_2O_2 conv. (%)	PO sel. (%)	PO yie. (%)	H_2O_2 eff. (%)
TS-1-E-80-170	35.6	93.3	27.2	81.9
TS-1-C-80-170	17.4	90.6	13.8	83.4
TS-1-E-170	32.6	91.1	23.2	83.2

Reactions conditions: catalyst, 0.03 g; H_2O_2 (30 wt.%), 0.03 mol; solvent MeOH, 10 mL; temperature, 313 K; time, 1 h. By-products: 1-methoxypropan-2-ol, 2-methoxypropan-1-ol, and 1,2-propanediol.

Table S6 Ti species and their quantities in different TS-1 samples.

Catalyst	Total Ti amount [a] (×10^{-2} mmol/g catalyst)	Ti-site	Ti-site amount [b] (×10^{-2} mmol/g catalyst)
TS-1-E-80-170	61.9	“TiO_4”	18.0
		$Ti(OH_2)(OSi)_3(OSiOH)_2$	43.9
TS-1-C-80-170	32.5	“TiO_4”	6.0
		$Ti(H_2O)_2(OH)_2(OSi)_2$	24.7
		Anatase-TiO_2	1.8
TS-1-E-170	64.2	“TiO_4”	17.0
		$Ti(OH_2)(OSi)_3(OSiOH)_2$	36.9
		Anatase-TiO_2	10.3

a. Calculated by ICP-OES results. b. Calculated by UV-Raman, UV-vis, and ICP-OES results.

Calculating turnover number (TON) of different catalysts and Ti species

Catalytic activity of different catalysts and Ti species are evaluated by turnover number (TON). TON of different catalysts and Ti species are calculated by the following formula. (Anatase-TiO$_2$ has no propylene epoxidation activity, so TON of Anatase-TiO$_2$ is 0.

$$TON = \frac{n(PO)}{n(Ti)} = \frac{Y(PO) \times n_0(H_2O_2)}{n(Ti)}$$

$$TON_{TS-1-E-80-170} = \frac{n(PO)_{TS-1-E-80-170}}{n(Ti)_{TS-1-E-80-170}} = \frac{0.272 \times 0.03\, mol}{0.03\, g \times 61.9 \times 10^{-5}\ mol\, g^{-1}} = 439$$

$$TON_{TS-1-C-80-170} = \frac{n(PO)_{TS-1-C-80-170}}{n(Ti)\ _{TS-1-C-80-170}} = \frac{0.138 \times 0.03\, mol}{0.03\, g \times 32.5 \times 10^{-5}\ mol\, g^{-1}} = 425$$

$$TON_{TS-1-E-170} = \frac{n(PO)_{TS-1-E-170}}{n(Ti)_{TS-1-E-170}} = \frac{0.232 \times 0.03\, mol}{0.03\, g \times 64.2 \times 10^{-5}\ mol\, g^{-1}} = 361$$

$$n(PO)_{TS-1-E-80-170} = n(Ti)_{TS-1-E-80-170} \times TON_{TS-1-E-80-170}$$

$$= n("TiO_4")_{TS-1-E-80-170} \times TON("TiO_4") + n(Ti(OH_2)(OSi)_3(OSiOH)_2)_{TS-1-E-80-170}$$

$$\times TON(Ti(OH_2)(OSi)_3(OSiOH)_2)$$

$$= 0.03\, g \times 18.0 \times 10^{-5}\ mol\, (g\,)^{-1} \times TON("TiO_4") + 0.03\, g \times 43.9 \times 10^{-5}\ mol\, (g\,)^{-1}$$

$$\times TON(Ti(OH_2)(OSi)_3(OSiOH)_2) = 8.16 \times 10^{-3}\, mol$$

$$18.0 \times TON("TiO_4") + 43.9 \times TON(Ti(OH_2)(OSi)_3(OSiOH)_2) = 27200 \qquad (1)$$

$$n(PO)_{TS-1-C-80-170} = n(Ti)_{TS-1-C-80-170} \times TON_{TS-1-C-80-170}$$

$$= n("TiO_4")_{TS-1-C-80-170} \times TON("TiO_4") + n("TiO_6")_{TS-1-C-80-170} \times TON("TiO_6") +$$

$$n(Anatase - TiO_2)_{TS-1-C-80-170} \times TON(Anatase - TiO_2)$$

$$= 0.03\, g \times 6.0 \times 10^{-5}\ mol\, g^{-1} \times TON("TiO_4") + 0.03\, g \times 24.7 \times 10^{-5}\ mol\, g^{-1}$$

$$\times\ TON("TiO_6")\ =\ 4.14 \times 10^{-3}$$

$$6.0 \times TON("TiO_4") + 24.7 \times TON("TiO_6") = 13800 \qquad (2)$$

$$n(PO)_{TS-1-E-170} = n(Ti)_{TS-1-E-170} \times TON_{TS-1-E-170}$$

$$= n("TiO_4")_{TS-1-E-170} \times TON("TiO_4") + n(Ti(OH_2)(OSi)_3(OSiOH)_2)_{TS-1-E-I70}$$

$$\times TON(Ti(OH_2)(OSi)_3(OSiOH)_2) + n(Anatase - TiO_2)_{TS-1-E-170} \times TON(Anatase - TiO_2)$$

$$= 0.03\, g \times 17.0 \times 10^{-5}\ mol\ \ g^{-1} \times TON("TiO_4") + 0.03\, g \times 36.9 \times 10^{-5}\ mol\, g^{-1}$$

$$\times TON(Ti(OH_2)(OSi)_3(OSiOH)_2) = 6.96 \times 10^{-3}\, mol$$

$$17.0 \times TON("TiO_4") + 36.9 \times TON(Ti(OH_2)(OSi)_3(OSiOH)_2) = 23200 \qquad (3)$$

Solve the system of equations composed of (1), (2), and (3)

$$\begin{bmatrix} 43.9 & 0 & 18.0 \\ 0 & 24.7 & 6.0 \\ 36.9 & 0 & 17.0 \end{bmatrix} \begin{bmatrix} TON(Ti(OH_2)(OSi)_3(OSiOH)_2) \\ TON("TiO_6") \\ TON("TiO_4") \end{bmatrix} = \begin{bmatrix} 27200 \\ 13800 \\ 23200 \end{bmatrix}$$

TON(“TiO_4”)=180, TON($Ti(H_2O)_2(OH)_2(OSi)_2$)=515, TON($Ti(OH_2)(OSi)_3(OSiOH)_2$) = 546.

Table S7 Comparison of propylene epoxidation activity among various catalysts.

	Modifier	n(H_2O_2) [mol]	Catalyst mass [g]	T [°C]	C_3H_6 pressure [Mpa]	Time [h]	H_2O_2 Conv. [%]	PO Sel. [%]	PO Yie. [%]	PO formation rate [g_{PO} g_{cat}^{-1} h^{-1}]^a	Ref
TS-1-E-80-170	—	0.030	0.03	40	0.4	1	35.6	93.3	27.2	15.78	This work
m-TS-1	—	0.102	0.10	30	0.6	1	—	98.6	ca. 12.2	ca. 7.08	4
ML-TS-1	TPAOH	0.102	0.10	30	0.6	1	—	99.2	ca. 27.6	ca. 16.01	4
TS-1-P	—	0.120	0.40	50	0.6	2	85.6	64.9	55.5	4.81	6
TS-1-A	Amino-2-propanol	0.120	0.40	50	0.6	2	79.7	79.2	63.1	5.51	6
TS-1	—	0.040	0.50	45	0.4	1.5	74.9	82.5	59.9	1.86	7
HTS-1-4	Phenolic Resin	0.040	0.50	45	0.4	1.5	98.3	93.6	89.7	2.78	7
TS-1	—	0.027	0.08	45	0.6	1	33.7	98.6	30.9	6.03	8
TS-1-TPAOH	TPAOH	0.027	0.08	45	0.6	1	99.1	99.3	96.0	18.79	8
TS-1-EOA+T	Ethanolamine+TPABr	0.027	0.08	45	0.6	1	99.7	99.2	97.4	19.07	8
TS-1	—	0.026	0.50	50	0.4	1	87.2	92.9	81.0	2.44	9
NTS-1	—	0.026	0.50	50	0.4	1	92.6	96.1	88.9	2.68	9
HTS-1	NH_4F	0.026	0.50	50	0.4	1	98.4	97.6	96.0	2.90	9
µmTS-1	—	0.088	0.15	40	0.6	1	36.1	90.7	28.6	9.73	10
170-16h	NaOH+TPABr	0.088	0.15	40	0.6	1	17.7	99.5	10.4	3.54	10
170-16h-NH_4NO_3	NH_4NO_3	0.088	0.15	40	0.6	1	63.5	94.1	54.9	18.69	10
TPAOH-170-16h	NaOH+TPAOH	0.088	0.15	40	0.6	1	50.1	96.3	45.3	15.42	10

a. PO formation rate = $M(PO)\cdot n(PO)/(m_{cat}\cdot time)$ = $M(PO)\cdot Y(PO)\cdot n(H_2O_2)/(m_{cat}\cdot time)$

References

1. Goedecker, S.; Teter, M.; Hutter, J., Separable dual-space Gaussian pseudopotentials. *Phys. Rev. B* **1996**, *54*, 1703-1710.

2. Perdew, J. P.; Burke, K.; Ernzerhof, M., Generalized Gradient Approximation Made Simple. *Phys. Rev. Lett.* **1996**, *77*, 3865-3868.

3. Grimme, S.; Antony, J.; Ehrlich, S.; Krieg, H., A consistent and accurateab initioparametrization of density functional dispersion correction (DFT-D) for the 94 elements H-Pu. *J. Chem. Phys.* **2010**, *132*, 154104.

4. Wang, Y.; Yang, H.; Zuo, Y.; Tian, D.; Hou, G.; Su, Y.; Feng, Z.; Guo, X.; Li, C., New penta- and hexa-coordinated titanium sites in titanium silicalite-1 catalyst for propylene epoxidation. *Appl. Catal., B* **2023**, *325*, 122396.

5. D. H.Olson; G. T. Kokotailo; S. L. Lawton, Crystal Structureand Structure-Related Properties of ZSM-5. *J. Phys. Chem.* **1981**, *85*, 2238-2243.

6. Wang, G.; Li, Y.; Lin, L.; Guo, Y.; Zhang, C.; Li, G.; Feng, Z.; Guo, H., Liquid-Phase Epoxidation of Propylene with H_2O_2 over TS-1 Zeolite: Impurity Formation and Inhibition Study. *Ind. Eng. Chem. Res.* **2021**, *60*, 12109-12122.

7. Wang, B.; Zhu, Y.; Han, H.; Qin, Q.; Zhang, Z.; Zhu, J., Preparation and Catalytic Performance in Propylene Epoxidation of Hydrophobic Hierarchical Porous TS-1 Zeolite. *Catal. Lett.* **2022**, *152*,

3076-3088.

8. Liu, M.; Wei, H.; Li, B.; Song, L.; Zhao, S.; Niu, C.; Jia, C.; Wang, X.; Wen, Y., Green and efficient preparation of hollow titanium silicalite-1 by using recycled mother liquid. *Chem. Eng. J.* **2018**, *331*, 194-202.

9. Li, Y.; Fan, Q.; Li, Y.; Feng, X.; Chai, Y.; Liu, C., Seed-assisted synthesis of hierarchical nanosized TS-1 in a low-cost system for propylene epoxidation with H_2O_2. *Appl. Surf. Sci.* **2019**, *483*, 652-660.

10. Miao, C.; Zhu, Q.; Yi, Y.; Su, J.; He, N.; Liu, J.; Guo, H., Gas-Phase Epoxidation of Propylene with Hydrogen Peroxide Vapor: Effect of Modification with NaOH on TS-1 Titanosilicate Catalyst in the Presence of Tetra-propylammonium Bromide. *Ind. Eng. Chem. Res.* **2019**, *58*, 11739-11749.